GA–A22887

WAVELENGTH CALIBRATION OF THE CHARGE EXCHANGE RECOMBINATION SPECTROSCOPY SYSTEM ON THE DIII–D TOKAMAK

by
P. GOHIL, K.H. BURRELL, R.J. GROEBNER, K. HOLTROP,
K.H. KAPLAN, P. MONIER-GARBET

JUNE 1998

DISCLAIMER

GA–A22887

WAVELENGTH CALIBRATION OF THE CHARGE EXCHANGE RECOMBINATION SPECTROSCOPY SYSTEM ON THE DIII–D TOKAMAK

by
P. GOHIL, K.H. BURRELL, R.J. GROEBNER, K. HOLTROP, K.H. KAPLAN, P. MONIER-GARBET*

This is a preprint of a paper to be presented at the Twelfth Topical Conference on High-Temperature Plasma Diagnostics, June 7–11, 1998, Princeton, New Jersey and to be published in *Review of Scientific Instruments*.

***Association EURATOM-CEA, Centre d'Etudes de Cadarache, Cedex, France**

Work supported by the U.S. Department of Energy under Contract No. DE-AC03-89ER51114

GA PROJECT 3466
JUNE 1998

ABSTRACT

A wavelength calibration of all the detectors on the charge exchange recombination spectroscopy (CER) system is performed after every plasma discharge on the DIII–D tokamak. This is done to insure that the rest wavelength position of the C VI 5290.5 Å charge exchange line on the detector is accurately known so that the Doppler shift of the spectral line emitted during the discharge can be used for measurements of plasma rotation. In addition, this calibration provides a check on the spectral dispersion needed to determine the ion temperature. The reference spectra for the calibration are Ne I lines created by neon capillary discharge lamps contained within specially designed, diffuse reflectors. The Ne I lines at 3520.4720 Å, 5274.0393 Å, 5280.0853 Å, 5298.1891 Å, and 5304.7580 Å are used in this work. The location of these lines on the linear detectors can be determined to an accuracy of 0.1 pixel, which corresponds to a plasma rotation accuracy of 1.2 km/s and 0.7 km/s for the central and edge rotation measurements, respectively. Use of oppositely directed views of the plasma at the same major radius have been used to verify that the nominal 5290.5 Å wavelength of the C VI ($n = 8 \rightarrow 7$) multiplet is the correct wavelength for the line emitted owing to charge exchange excitation.

1. INTRODUCTION

The charge exchange recombination spectroscopy (CER) system is the prime diagnostic for measurements of the ion temperature, plasma rotation and impurity density in DIII–D.[1] Precise knowledge of these plasma quantities is needed for accurate determination of the radial electric field, E_r, especially at the plasma edge. In particular, the plasma rotation, both toroidal and poloidal, are key quantities in the determination of E_r. Knowledge of the E_r profile is essential for evaluation of the $E \times B$ shearing rate,[2] which is used in determining the effectiveness of non-linear decorrelation and linear stabilization of turbulent eddies by the $E \times B$ velocity shear.[3] Notably, increased local gradients in the radial profile of E_r have led to the formation of transport barriers at the plasma edge (H–mode transition)[4] and in the plasma core (internal transport barriers).[3] Therefore, accurate plasma rotation measurements are required across the entire plasma radius.

In DIII–D, the plasma rotation is determined predominantly from measurements of the Doppler shifted line-center wavelength of the nominal 5290.5 Å ($n = 8 \rightarrow 7$) charge exchange line of the C VI impurity ions. Measurements of the wavelength shifts are facilitated by performing a wavelength calibration of the complete CER system after every plasma discharge on DIII–D. This also provides spectral dispersion for all the detection systems. The reference spectra for the calibrations are Ne I lines obtained from the output of neon capillary discharge lamps contained within custom designed housings. These housings were constructed by Labsphere[5] and consist of hollow cavities with diffusely reflecting walls. These housings will be referred to as labspheres in the rest of this paper. This paper describes details of the hardware, operational requirements, analysis of the measured spectra, and determination of the rest wavelength of the C VI ($n = 8 \rightarrow 7$) charge exchange line.

2. MECHANICAL ASSEMBLIES

The CER system couples light from the plasma to the spectrometers using fiber optics. The detectors in the system consist of RETICON linear detectors used in conjunction with high-voltage microchannel plates. The 40 CER spatial channels are distributed over five machine ports, each with their own viewing optics to form vertically or horizontally viewing arrays inside the DIII–D vessel. The mechanical hardware for the calibration systems are all located at the machine ports. Therefore, the emission from five different neon lamp and labsphere combinations are needed to cover all the 40 spatial channels. Each of the five lamp/labsphere assemblies are different, but they all adhere to the same design concept of a neon lamp placed inside a labsphere diffusive housing with a single aperture through which the neon light emanates and is directed onto the optical fibers, which define the various CER spatial channels. Each labsphere housing is specifically designed according to: (a) the geometrical layout of the optical fibers and the viewing optics, and; (b) the space constraints around the ports. Figure 1 shows a diagram of a typical labsphere arrangement. The labsphere material consists entirely of Spectralon[5] which has a perfectly Lambertian reflecting surface with a reflectance of 99% between 4000–8000 Å. These low losses and diffusive reflections ensured an even distribution of light emission from the labsphere apertures onto the optical fibers. Furthermore, Spectralon is thermally stable to the temperature increases in the proximity of the DIII–D vessel during the vessel's baking cycle.

The light sources consist of neon capillary discharge lamps producing low intensity, narrow lines and specifically constructed for spectral calibration purposes.[6] The lamps are used in conjunction with AC power supplies. The operating current is 6 mA and the dissipated power is 1.6 W. The lamps are mounted in the labspheres such that the full irradiance from the lamp is contained within the labsphere housing apart from the output through the labsphere aperture. A quartz Tungsten halogen lamp is also

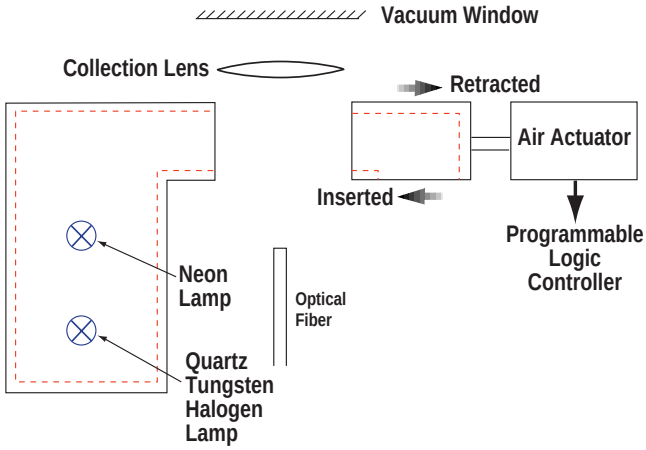

Fig. 1. Diagram of a typical labsphere/lamp configuration installed around the viewing optics of each CER port.

mounted inside each labsphere for the purpose of performing white light calibrations of the detector response and is not used during the shot-to-shot wavelength calibration.

For all but one of the lamp/labsphere combinations, the labspheres are split into two parts (see Fig. 1). One part is statically mounted and houses the light sources and the other part consists of the aperture cap which couples with the static housing and is actuated between shots. In the case of one lamp/labsphere combination, the labsphere is one whole unit which is actuated as one assembly into the viewing path of the fibers. The labsphere caps are normally completely retracted away from the optical path of plasma light incident on the collection optical fibers. However, after each plasma discharge, the labspheres are inserted into the optical path such that the optical fibers view directly into the labsphere caps. The neon lamps are then illuminated and the neon light is collected by the fibers. The labspheres are mounted on air actuated linear thrusters with viton seals for high temperature operations. The length of the stroke is adjusted using externally mounted bumpers. Externally mounted mechanical microswitches are positioned to be activated at the limits of the stroke. These limit switches are incorporated into the logic control circuitry and provide feedback on the position of the labsphere.

3. CONTROL LOGIC

All five wavelength calibration systems are interfaced with the DIII–D vacuum system programmable logic controller (PLC). This PLC is one of the primary mechanisms for coordinating various operations and interlocks for the DIII–D vacuum system. It continuously monitors and controls a variety of instrumentation and devices such as gate valves, shutters, turbo-pumps, air compressors, ion gauges and temperature monitors. In addition, the PLC controls many of the vacuum related processes such as glow discharge cleaning and heating and cooling of the vessel. The PLC controls the operation of the labspheres caps and the neon lamps in conjunction with the above activities. The labsphere caps' motion and lamps' illumination can be controlled manually. However, during a DIII–D shot cycle these operations are automatically sequenced by the PLC during the shot cycle. The automatic sequence is triggered by an end-of-shot trigger produced by the DIII–D timing generator. Ten seconds after this trigger, the labsphere caps are inserted into the optical path of the collection fibers. After a further 50 s delay, the neon lamps for all the labspheres are simultaneously turned on for a duration of 100 s. This allows time for the lamps to stabilize and for the data to be acquired. Then the lamps are turned off and the labsphere caps are retracted. The labsphere caps are interlocked to be retracted during the tokamak discharges and also during baking of the vessel. The neon lamps are interlocked to be turned off during any time the toroidal and poloidal field coils and the ohmic coils are energized.

4. CALIBRATION SPECTRA

The neon spectral lamps produce discrete lines of Ne I in the UV, visible and IR. The characteristics of the observed spectra depend on the spectrometer dispersion and operational setting (first or second order) and on the detector response. Figures 2 and 3 show typical spectra for two spatial channels, one is for the first order and the other is for the second order. The Ne I lines are at 3520.4720 Å, 5274.0393 Å, 5280.0853 Å, 5298.1891 Å, and 5304.7580 Å.[7] The detectors for these spectra are RETICON linear diode arrays used in conjunction with high voltage microchannel plates, which are not sensitive to IR wavelengths for the second order settings of some of the spectrometers. However, the main line in the second order spectrum is a third order overlap of a Ne I UV line at 3520.4720 Å. The spectra shown are the result of an average of 100 frames with an integration time of 50 ms per frame. Light sources using other elements were investigated, e.g., Xe, He, Ar, but these did not provide adequately bright lines in the wavelength range of interest. The spectra are fitted using an analysis code utilizing non-linear least-square Gaussian fits to the various peaks. Overall, the determination of the fiducial locations for the C VI rest wavelength is accurate to 0.1 pixel on the RETICON array.

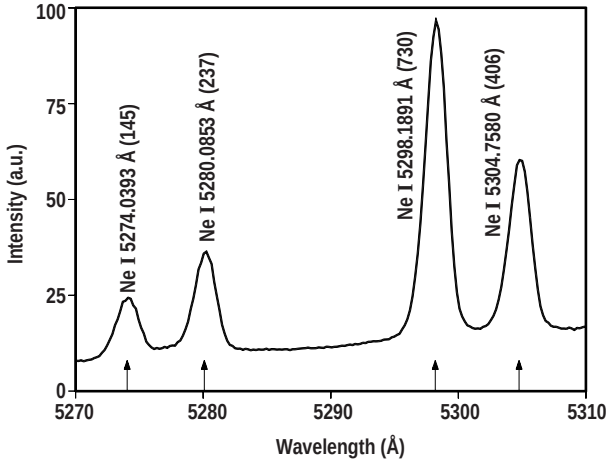

Fig. 2. Spectrum of Ne I lines observed in the first order. The wavelength of each line is labeled and its peak is noted along the x-axis. The relative amplitude of each line is stated within the brackets (in arbitrary units).

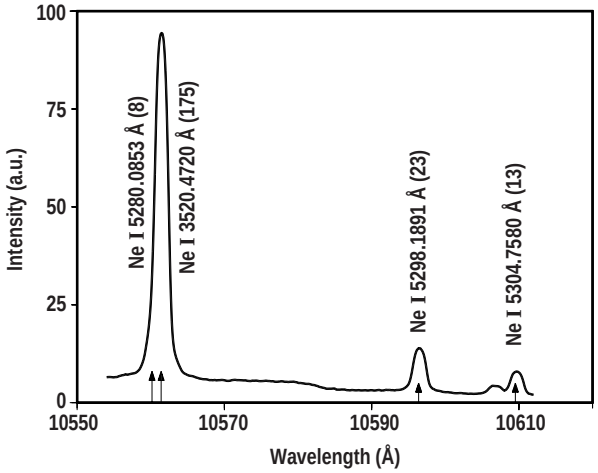

Fig. 3. Spectrum of Ne I lines in the second order. Same legend as in Fig. 2.

5. WAVELENGTH ANALYSIS

The neon spectra provide spectral dispersion and determinations of the relative rotations for the CER chords for every plasma discharge. However, for an absolute measurement of the plasma rotation, the rest wavelength of the C VI (n = 8→7) charge exchange line needs to be known. The rest wavelength of the C VI line has been determined from analysis of the toroidal rotation of two oppositely viewing tangential chords, labeled T7 and T8. These chords are mounted on the same spectrometer and observed by the same detector assemblies. Chord T7 views at a major radius of 220.2 cm and T8 views at 220.4 cm, and so both chords essentially view the same major radius. The Doppler shift for each chord is given by:

$$\lambda_i - \lambda_o = \frac{\nu_\phi \lambda_o}{c} \cos\theta_i \quad , \tag{1}$$

where λ_i is the Doppler shifted wavelength for the ith chord, ν_ϕ is the toroidal rotation speed, λ_0 is the rest wavelength of the line and θ_i is the angle between the line of sight of the chord and the toroidal direction.

The wavelength, λ_i , for a particular chord can be determined from the pixel difference between the measured line and the neon line and the dispersion by:

$$\lambda_i = D_i\left(P_i - P_{Ne,i}\right) + \lambda_{Ne} \quad , \tag{2}$$

where D_i is the dispersion in Å/pixel, P_i is the pixel location of the line center of the charge exchange line, $P_{Ne,i}$ is the pixel location of the main neon line and λ_{Ne} is the wavelength of the main neon line. Combining Eqs. (1) and (2) for both the oppositely viewing chords T7 and T8 gives:

$$D_7\left(P_7 - P_{Ne,7}\right) + \lambda_{Ne} - \lambda_o = \frac{\nu_\phi \lambda_o}{c} \cos\theta_7 \quad , \tag{3}$$

and

$$D_8\left(P_8 - P_{Ne,8}\right) + \lambda_{Ne} - \lambda_o = \frac{\nu_\phi \lambda_o}{c}\cos\theta_8 \quad , \tag{4}$$

which, by eliminating $\frac{\nu_\phi \lambda_o}{c}$, gives

$$\begin{aligned} P_7 - P_{Ne,7} = {} & \frac{D_8}{D_7}\frac{\cos\theta_7}{\cos\theta_8}\left(P_8 - P_{Ne,8}\right) \\ & + \frac{\lambda_o - \lambda_{Ne}}{D_7}\left(1 - \frac{\cos\theta_7}{\cos\theta_8}\right) \end{aligned} \quad , \tag{5}$$

Therefore, a plot of $(P_7–P_{Ne,7})$ against $(P_8–P_{Ne,8})$ gives the ratio $\cos\theta_7/\cos\theta_8$, determined from the slope, and the value of λ_0, determined from the offset from the origin. The Ne I 5298.1981 Å line was used as λ_{Ne}.

Wavelength analysis for T7 and T8 was carried out for five different discharges. Figure 4 shows the rotation speeds for the oppositely viewing chords T7 and T8 as a function of time for one discharge. The different values correspond to increasing plasma rotation with time during neutral beam heating. Similarly, Fig. 5 shows the same data where the rotation velocities of T7 and T8 are plotted against each other to determine their consistency. The rotation velocities are the line-of-sight values and contain a geometric factor defined by the cosine of the angle θ_i described in Eq. (1). The solid line represents the linear least square fit to the data. The slope of the line should be $\cos\theta_7/\cos\theta_8$ and the intercept should go through the origin. The fit to the slope gives $–0.987 \pm 0.011$ for the ratio of $\cos\theta_7/\cos\theta_8$. The intercept has a value of 0.735 ± 0.977 km-s^{-1} which is within the error for passage through the origin. Furthermore, the angles θ_7 and θ_8 have

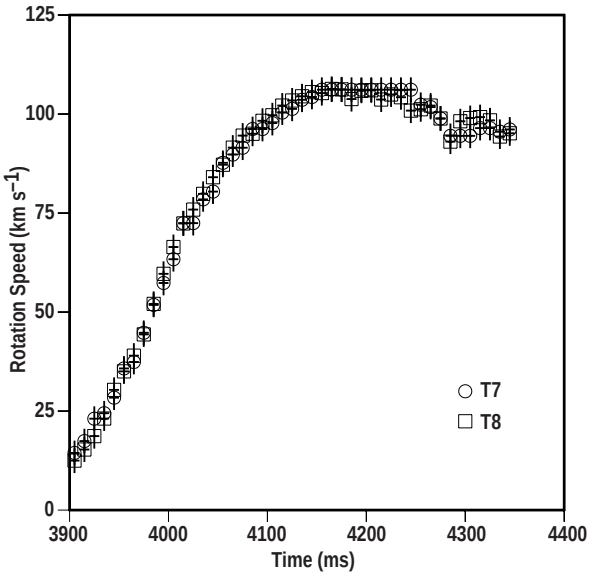

Fig. 4. Rotation speeds of T7 and T8 as a function of time. (Plasma discharge No. 85494.)

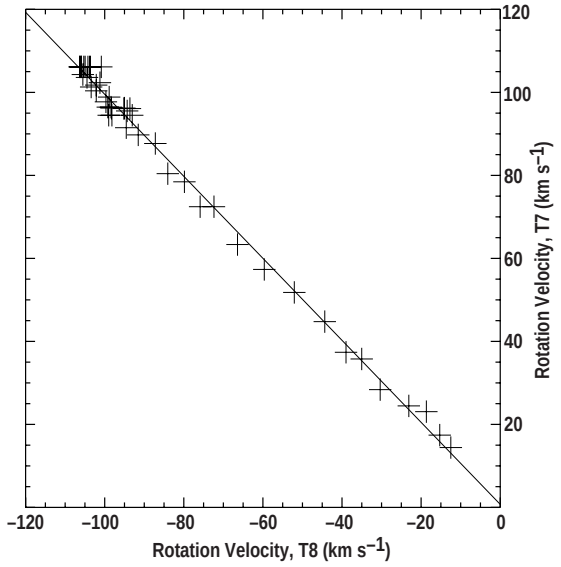

Fig. 5. Line-of-sight rotation velocities of T7 and T8 plotted against each other.

also been determined independently from spatial calibration measurements inside the DIII–D vessel. The geometric measurements give a ratio of $\cos\theta_7/\cos\theta_8 = -0.978$. The values of $\cos\theta_7/\cos\theta_8$ from the rotation analyses and geometric measurements agree within the experimental error and so further validate the rotational analyses. Figure 6 shows the values of $(P_7–P_{Ne,7})$ and $(P_8–P_{Ne,8})$ for the same discharge. The solid line shows the linear least square fit to the data. The fit to the gradient has a value -0.997 ± 0.011. This represents the ratio D_8/D_7 $\cos\theta_7/\cos\theta_8$. D_7 and D_8 are the spectral dispersions determined from the neon lines with $D_7 = 0.2037$ Å/pixel and $D_8 = 0.2055$ Å/pixel. This then gives a mean value of –0.988 for $\cos\theta_7/\cos\theta_8$ which is consistent with the slope of Fig. 5 within the error bar. The offset has a value of -75.053 ± 0.245. This results in a determination of the rest wavelength of the C VI ($n = 8 \rightarrow 7$) line as $\lambda_0 = 5290.51$ Å ± 0.03 Å. Taking the mean of the analysis results from the five different discharges gives $\lambda_0 = 5290.52$ Å ± 0.05 Å and $\cos\theta_7/\cos\theta_8 = -0.981 \pm 0.021$. This is consistent with the tabulated value of 5290.53 Å for the centroid of the C III ($n = 8 \rightarrow 7$) multiplet.[8]

The collision-energy-dependent cross-section effects on the plasma rotation were examined.[9] These effects lead to changes in the shape of the observed charge exchange spectra as a result of changes in the effective emission rates caused by the velocity distribution of the ions. The formalism for the cross-section effects given in Ref. 8 was used. For the chord geometry of CER chords

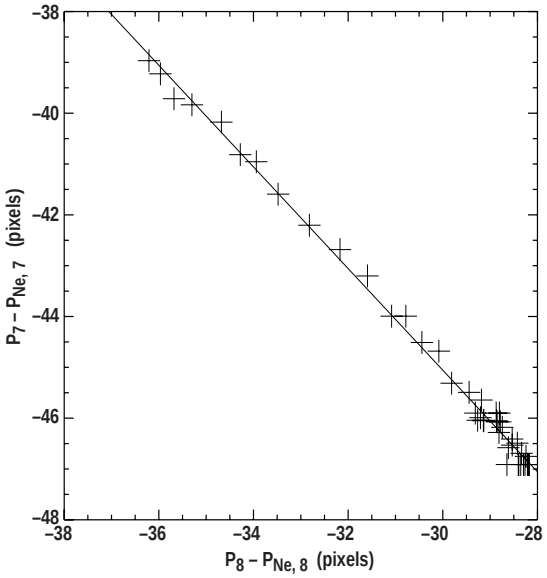

Fig. 6. Plot of difference $(P_7–P_{Ne,7})$ as a function of $(P_8–P_{Ne,8})$ for the oppositely viewing chords T7 and T8. P7 and P8 are the pixel locations of the line-center of the C VI ($n = 8 \rightarrow 7$) CER line for T7 and T8 respectively and $P_{Ne,7}$ and $P_{Ne,8}$ are the pixel locations of the Ne I 5298.1891 Å line in the T7 and T8 spectra respectively.

T7 and T8 and beam energies of 37.5 keV/amu and ion temperatures of 1 keV (the maximum values attained by T7 and T8) the cross-section effects lead to a change in toroidal plasma rotation by 2.6 km s^{-1} in the case of the C VI ($n = 8 \rightarrow 7$) charge exchange line. Note that this is the maximum effect and the effect on the rotation is much less at the lower temperatures applicable to most of the data points shown in Fig. 6. This maximum rotation change is very close to the limiting resolution of 1.2 km s^{-1} of the rotation measurement possible from the observed spectra. If the cross-section effects are included then the analyses gives the rest wavelength as $\lambda_0 = 5290.52 \pm 0.06$ Å. Therefore, the error introduced by the cross-section effects is small.

ACKNOWLEDGMENTS

This work was supported by the U.S. Department of Energy under Contract No. DE-AC03-89ER51114.

REFERENCES

[1]P. Gohil, *et al.*, in Fusion Engineering (Proc. 14th Symp. San Diego, 1991).Vol. 2, IEEE, New York 1199 (1992).

[2]T.S. Hahm and K.H. Burrell, Phys. Plasmas **2** 1648 (1995).

[3]K.H. Burrell, Phys. Plasmas **4** 1499 (1997).

[4]P. Gohil, K.H. Burrell, T. N. Carlstrom, Nucl. Fusion **38** 93 (1998).

[5]Labsphere, P.O. Box 70, Shaker Street, North Sutton, NH 03260.

[6]Oriel Corporation, 250 Long Beach Blvd., Stratford, Connecticut 06497.

[7]A.P. Striganov and N.S. Sventitskii, Tables of Spectral Lines of Neutral and Ionized Atom, (IFI/Plenum, New York , 1968).

[8]J.D. Garcia, J.E. Mack, J. Opt. Soc. Am. **55** 654 (1965).

[9]M. von Hellermann, *et al.*, Plasma Phys. Control. Fusion **37** 71 (1995).